J Infrared Milli Terahz Waves (2012) 33:183–191
DOI 10.1007/s10762-011-9857-7

Terahertz time-domain-spectroscopy system using a 1 micron wavelength laser and photoconductive components made from low-temperature-grown GaAs

A. Bičiūnas · J. Adamonis · A. Krotkus

Received: 3 May 2011 / Accepted: 21 November 2011 /
Published online: 2 December 2011

Abstract A terahertz time-domain spectroscopy (TDS) system based on a femtosecond Yb: KGW laser, photoconductive emitters and detectors made from as-grown and from annealed at moderate temperatures (~400°C) low-temperature-grown GaAs (LTG GaAs) layers was demonstrated. The measured photoconductivity of these layers increased linearly with the optical power, showing that transitions from the defect band to the conduction band are dominant. The largest amplitude THz pulse with a useful signal bandwidth reaching 3 THz and its signal-to-noise ratio exceeding 50 dB was emitted by the device made from the LTG GaAs layer annealed at 420°C temperature. The detector made from this material was by an order of magnitude less sensitive than conventional GaBiAs detectors.

Keywords Terahertz · Optical pump – THz probe · LTG GaAs · 1 μm wavelength time-domain-spectroscopy · Optoelectronic terahertz components

1 Introduction

Ultrafast photoconductive switches with integrated microstrip antennas are widely used for terahertz frequency range emitters and detectors in the time-domain-spectroscopy systems as well as for the continuous wave THz signal generation in photomixers. Most commonly used switches are based on an epitaxial GaAs layers grown by molecular-beam-epitaxy (MBE) technique at relatively low (200°C to 300°C) substrate temperatures and afterwards annealed at 600°C or higher temperatures [1, 2]. Besides the unique set of parameters – a high electrical breakdown field, large resistivity, and carrier lifetime shorter than 1 ps – this material has the additional advantage of an absorption edge compatible with the quantum energy of a Ti:sapphire laser (~1.5 eV). This property encouraged the first successful development of commercial THz-TDS systems.

A. Bičiūnas (✉) · J. Adamonis · A. Krotkus
Center for Physical Sciences and Technology, A. Goštauto 11, LT-01108 Vilnius, Lithuania
e-mail: biciunas@pfi.lt

Recently, several types of femtosecond solid-state and fiber lasers emitting at the near infrared wavelengths between 1 and 1.55 μm have been developed [3, 4]. These lasers are more compact and more efficient, thus, potentially, they are a cheaper alternative to the Ti: sapphire lasers. THz-TDS systems based on these lasers could stimulate a wider range of implementations. However, the excitation of THz components made from annealed LTG GaAs with 1 μm and longer wavelength laser pulses is inefficient since the energy bandgap of GaAs is larger than the corresponding photon energy quanta and the two-photon absorption processes are not efficient enough. This restriction led to increasing interest in the study of semiconductor materials possessing a narrower energy bandgap. Materials such as InGaAs [5], GaBiAs [6], GaSbAs [7], and multi-layer structures including ErAs nanoparticles [8, 9] were investigated as a basis of the THz devices operating at 1 μm and 1.55 μm wavelengths. However, the increase of optical absorption in these detectors was always achieved at the cost of a reduced dark resistivity and a relatively low breakdown voltage.

In our previous work it was demonstrated that optoelectronic THz range components activated with 1 μm wavelength lasers can be manufactured from as-grown and annealed at moderate (~400°C) temperatures LTG GaAs layers [10]. These layers contain a large density (10^{19} to 10^{20} cm^{-3}) of excess As-related point defects, which are most probably arsenic-antisites (As_{Ga}). These defects create a defect band in the energy bandgap of GaAs. According to Ref. [11], the absorption coefficient at 1 μm wavelength, due to electron transitions from this band to the conduction band at the room temperature, can be quite large, of the order of 10^4 cm^{-1} magnitude. The dark conductivity of as-grown LTG GaAs is dominated by electron hopping in the defect band, resulting in quite low electron mobility. On the other hand, the mobility of photoexcited electrons in the conduction band should be comparable to that of the annealed material. Moreover, the breakdown field of the as-grown and moderately annealed layers is much larger that of layers annealed at higher temperatures (>600°C) [12]. This property enables applying large bias voltages to the emitters made from moderately annealed LTG GaAs, ensuring rather large optical-to-THz radiation conversion efficiencies.

In the present work, the performance of photoconductive switches based on the as-grown and annealed at moderate temperatures LTG GaAs was studied. These switches were implemented as emitters and detectors activated with 1 μm wavelength femtosecond pulses in the THz-TDS system. The characteristics of near-infrared absorption and non-equilibrium carrier lifetimes in these layers were investigated by optical pump – THz probe experiments and compared with rate equation calculations.

2 Experimental techniques

Epitaxial LTG GaAs layers grown on (100)-oriented SI GaAs substrates by the MBE system at 250°C substrate temperature with a growth rate of ~1 μm/h were studied. During the growth, layers were Be-doped in order to reduce the As_{Ga} ionization rate [13]. Other part of LTG GaAs layers were grown under the same conditions on the top of an AlAs/GaAs Bragg mirror with a maximum reflectance centered at 1 μm wavelength. The thickness of all LTG GaAs layers was 1.4 μm. Both non-annealed and annealed layers were studied. The latter were annealed for 90s in a rapid thermal annealing oven at temperatures ranging from 400°C to 500°C. Coplanar Hertzian dipole antennas were manufactured with a photoconducting gap of 10–15 μm between the Ti-Au electrodes from LTG GaAs layers grown on a SI GaAs substrate. In order to collimate the emitted THz radiation, all antennas were equipped with hemispherical high resistivity Si lenses.

We used the oscillator from a high repetition rate femtosecond laser system Pharos (Light Conversion Ltd.) as an optical pulse source for terahertz pulse generation. The latter was based on a directly diode-pumped Yb:KGW crystal. Kerr-lens mode-locking was used to generate optical pulses with a pulse duration of 70 fs at a wavelength of 1030 nm, spectral line-width (FWHM) of 22 nm and a pulse repetition rate of 76 MHz. The average output power of the oscillator was about 2 W. In the THz-TDS system, the laser beam was split into two parts of different intensity. The lower intensity beam (the power of ~20 mW) activated the photoconductive terahertz emitter and the higher intensity beam (the power of ~25 mW) activated the photoconductive THz pulse detector. The THz detector was made from a $Ga_{0.96}Bi_{0.04}As$ layer, grown by MBE at low temperature (280°C) on a semi-insulating (SI) (100)-oriented GaAs substrate [6, 14]. The electron trapping time in the detector material was shorter than 1 ps resulting in a Fourier transform spectra of the detected electromagnetic transients wider than 4 THz.

Additionally, for the optical pump – THz probe technique [15] a 1.9 mm diameter pinhole was used to overlap the THz pulse and the photoexcitation beam on the sample. The spot size of the pump beam was larger than the diameter of the pinhole, so that the THz beam was sampling a nearly uniformly photoexcited region. To maximize the transmitted power through the pinhole, the THz beam was focused before and collimated behind the pinhole by two hemispherical Teflon lenses. All measurements were performed at room temperature.

3 Theoretical model

To describe the excited charge density dependence on the optical excitation power we used the Shockley-Read-Hall model with the following assumptions. Only negative charge carrier excitation from deep As_{Ga} donor levels was considered. Since the Fermi level is pinned to the deep donor band lying at ~0.8 eV below the conduction band edge, the conduction band is considered to be almost empty in the absence of the photoexcitation. Only a small part of all As_{Ga} defects (N_{As}) are ionized due to their compensation by beryllium impurities or Ga vacancy acceptor states. The density of the ionized As_{Ga} defects is assumed to be the same as the density of Ga vacancies (N_{Va}), resulting in a small amount of initial electron trapping centers. The other charge carrier relaxation mechanisms such as the band-to-band radiative recombination as well as the Auger recombination were too weak to be considered.

The rate equation, describing the time-dependent concentration of the electrons (Δn) in the conduction band, can be expressed as follows:

$$\frac{d\,\Delta n}{dt} = (1-R)\cdot\sigma\cdot\frac{I}{h\omega_0}\cdot N_{As}^0 - \alpha\cdot\left(N_{As}-N_{As}^0\right)\cdot\ \Delta n, \tag{1}$$

where $N_{As}{}^0$ is the density of neutral point defects, R(~0.3) is the reflection coefficient of the incident laser pulse for GaAs, I is the time-dependent intensity of the laser pulse, $\hbar\omega_0$ is the photon energy, $\sigma = 1\ 10^{-16}$ cm^2 [16] and α are the photon capture cross-section and the electron capture rate for the As_{Ga} point defects, respectively. The latter parameter can be expressed as $\alpha = \sigma_s \cdot v_{th}$, where $\sigma_s = 1.1\ 10^{-13}$ cm^2 [17] is the capture cross-section of the defect and $v_{th} = 4\cdot 10^7$ cm·s^{-1} is the electron thermal velocity. For the electrons excited from a defect into the conduction band, the charge conservation equation can be written as follows:

$$N_{As}^0 = N_{As} - N_{Va} - \ \Delta n. \tag{2}$$

As a result, one obtains a nonlinear Riccati differential equation for time-dependent variable Δn, which, in general, cannot be solved analytically. This Eq. 1 was solved numerically and the solution was compared to the results of the optical pump – THz probe experiment.

4 Results and discussion

4.1 Optical pump – THz probe experiments

The optical pump – THz probe experiment was performed on an as-grown LTG GaAs layer on a SI GaAs substrate and on a bare GaAs substrate. Curves representing the dependence of the transmitted THz signal versus time delay for the as-grown LTG GaAs (black line) and for the bare GaAs substrate (grey line) are shown in Fig. 1. The change of the transmitted THz signal amplitude, induced by the photoexcitation of the sample, is caused by free-carrier absorption at THz frequencies and is proportional to the induced photoelectron conductance. The experimental curve corresponding to the LTG GaAs layer shows fast dynamics immediately after the excitation with the laser pulse, but the shape of the transient is dominated by a slowly changing component. This component is also observed in the curve corresponding to the bare GaAs substrate and it is increasing linearly with the increase of the optical pump intensity. The slowly changing dynamics of the optically-induced THz absorption, obscuring the interpretation of pump-and-probe measurements, is probably caused by the electron excitation from various deep donor levels in the 600 μm thick SI GaAs wafer. Long rise time of the substrate photoconductivity is, most probably, caused by the fact that 1.2 eV energy laser quanta excite the electrons with excess energies larger than the energy position of low-mobility X valleys. Similar THz conductivity transients caused by slow inter-valley redistribution of the photoexcited electrons have been observed before in germanium [18] and in several narrow-gap semiconductors [19].

To eliminate the effect of the GaAs substrate, the same experiment was repeated on the LTG GaAs layer grown on a Bragg reflector substrate. Figure 2 shows the shape of the optically induced THz absorption transient for an as-grown LTG GaAs sample. As it can be seen, the introduction of the Bragg reflector into the structure has completely removed the slowly changing transient component as well as the constant background signal. The FWHM

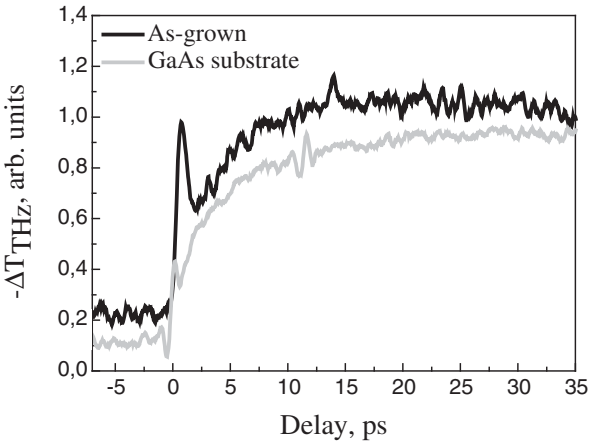

Fig. 1 Optical pump – THz probe measurements in an as-grown GaAs sample and in a bare GaAs wafer.

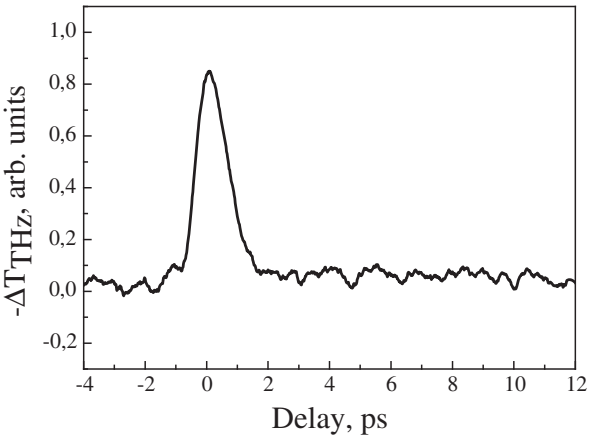

Fig. 2 Optically induced THz absorption transients measured for the LTG GaAs layer grown on the Bragg reflector.

duration of the induced THz absorption transient is ~0.9 ps and its rise and fall-times are similar. Thus, we can conclude that the electron lifetime in the layer is shorter than the temporal resolution of the experiment determined by the duration of the THz pulses (~0.6 ps).

We examined the induced THz absorption dependence on the near-infrared excitation level for three samples. The as-grown and annealed at 420°C and 450°C temperatures LTG GaAs samples were grown on the Bragg reflector. The experimental dependence for the as-grown sample is shown in Fig. 3 and is marked with squares. The experimental curves corresponding to the samples annealed at the temperatures of 420°C and 450°C temperatures are also shown in Fig. 3 and are marked with circles and triangles, respectively.

As it can be seen, the THz absorption for all the studied samples increases linearly with the increment of the photoexcitation level. This fact provides strong evidence that in the as-grown and moderately annealed LTG GaAs the photo-absorption at 1 μm wavelength is dominated by the electron transitions from the As-related defects rather than by two-photon or two-step absorption processes.

The largest THz absorption signal was obtained from the sample annealed at 420°C. It was slightly lower for the as-grown sample and approximately three times lower for the sample annealed at 450°C.

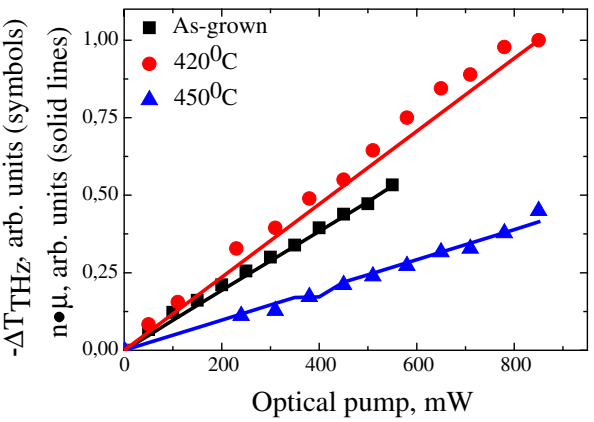

Fig. 3 Comparison of experimental and theoretical results. Points show experimental results of the THz transmittance peak value. Solid lines represent theoretical calculation of charge transient peak value multiplied by their mobility.

Since the THz absorption is proportional to the photoconductivity of the sample, the calculations performed in the previous section were used to evaluate the excitation level dependence on the optical pump intensity. Following Ref. [20], the As_{Ga} defect concentrations (N_{As}) for as-grown and annealed at 420°C and 450°C samples were assumed to be 20×10^{18} cm^{-3}, 4×10^{18} cm^{-3}, and 2×10^{18} cm^{-3}, respectively. Due to the annealing the concentration of the As_{Ga} defects decreases significantly, so the electron mobility was expected to increase. Thus, in the calculations performed for both annealed samples we assumed that the electron mobility is 5 times larger than that for the as-grown sample. The maximum charge excitation level corresponding to the non-equilibrium carrier density was evaluated to be $\sim1.4\times10^{15}$ cm^{-3} for the as-grown LTG GaAs. This value is too low to observe the saturation of the defect-to-band transitions.

The solid lines in Fig. 3 represent the results of the rate-equation calculations for the three studied samples. Good correspondence between calculated and experimental results is observed.

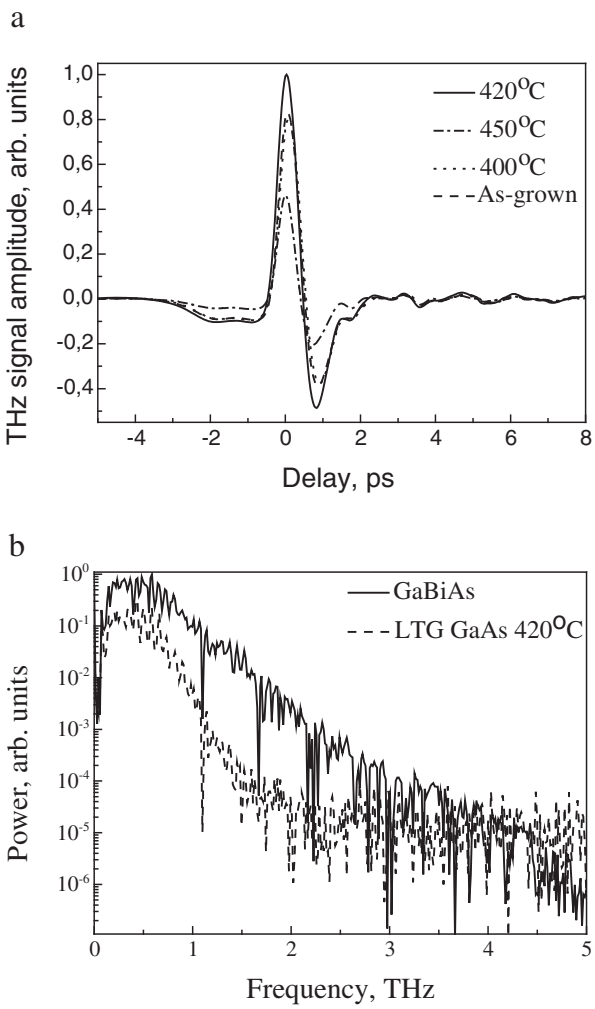

Fig. 4 THz pulses generated by photoconductive emitters made from as-grown and annealed at various temperatures LTG GaAs and sampled by the GaBiAs detector (**a**). Fourier spectrum of the THz pulse generated by LTG GaAs photoconductor annealed at 420°C and measured by the detectors made from the same material and from the epitaxial GaBiAs layer (**b**).

4.2 THz emitter and THz detector characterization

In this section, photoconductive switches manufactured from the materials studied in the former experiment will be described. For comparison, in the experiments we investigated additional photoconductive switches made from LTG GaAs annealed at 400°C, 500°C and higher temperatures. All the studied samples were grown without introduction of a Bragg reflector. All the switches were tested as THz pulse emitters in the THz-TDS system with the photoconductive detector made from the GaBiAs layer and illuminated with the average laser power of 20 mW for the THz pulse sampling. Experimental curves corresponding to THz pulses emitted by these switches are shown in Fig. 4a. THz pulses emitted by the switches made from as-grown and annealed at 400°C temperature samples were almost identical. The THz pulse with the largest amplitude was emitted by the device made from the layer annealed at the temperature of 420°C (solid line) in Fig. 4a. For this layer, the optically induced THz absorption was also the largest, as it was shown in the previous section. Photoconductive antennas made from the as-grown and the annealed at 450°C material emitted slightly lower-amplitude THz pulses. No THz pulses were detected from the devices annealed at 500°C and higher temperatures.

In the second part of this experiment, we compared the performance of the GaBiAs detector to that of the detector based on LTG GaAs, which was annealed at 420°C. The signal generated by the most efficient emitter (LTG GaAs annealed at 420°C) was detected by each of the detectors mentioned above. The Fourier-transform (FT) spectra of those signals are shown in Fig. 4b. The FT spectrum of the signal detected by the GaBiAs detector (solid line) has a useful bandwidth reaching 3 THz and its signal-to-noise ratio exceeds 50 dB. The FT spectrum corresponding to the photoconductive switch manufactured from the LTG GaAs (dashed line) is almost two times narrower and its sensitivity is ~15 times lower compared to the GaBiAs detector.

The most distinctive property of photoconductive THz emitters manufactured from LTG GaAs and annealed at moderate temperatures is their high breakdown voltage. An alternating meander-shaped voltage waveform with the amplitude varying between −150 V and +150 V was applied to a 10 μm wide photoconducting gap. The dependence of the THz pulse amplitude generated by the device annealed at 420°C on the bias voltage is shown in Fig. 5. The THz

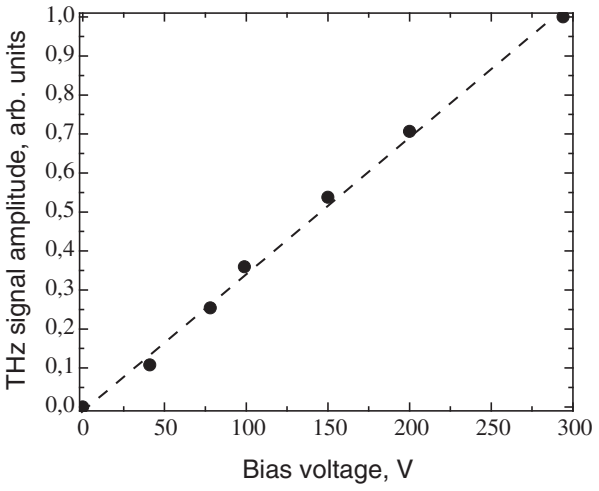

Fig. 5 Normalized THz signal amplitude generated by a terahertz emitter, annealed at 420°C, versus bias voltage.

pulse amplitude increases linearly with the increasing voltage. Thus, we can conclude that the electric breakdown field of the gap is larger than 150 kV/cm. This value is much higher than the value of the average electrical breakdown field of LTG GaAs annealed at high temperatures, which is typically around 50 kV/cm [12]. A significant increase of this parameter for as-grown and annealed at lower temperatures devices could be explained by the influence of the hopping conduction. The hopping current prevents the nucleation of the high-field domain in the anode region and leads to a more homogeneous electrical field distribution along the band gap. Thus, the avalanche breakdown in the device occurs at a higher voltage [12].

5 Conclusion

In conclusion, photoconductive antennas manufactured from as-grown and moderately annealed LTG GaAs layers activated by 1030 nm wavelength femtosecond duration laser pulses were used for terahertz pulse generation and detection. An optical pump – terahertz probe technique was used to study the ultrafast photoconductivity in these layers. It has been shown that this photoconductivity caused by the electrons excited from deep As_{Ga} donor levels is the highest for LTG GaAs annealed at the temperature of about 420°C. In the as-grown material it is lower because of the lower electron mobility, whereas higher annealing temperatures are leading to a significant reduction of the As_{Ga} defects.

As GaAs has a much larger energy bandgap than other semiconductors used for manufacturing optoelectronic THz components sensitive to 1 μm wavelength laser radiation, the investigated THz emitters could be biased to relatively large voltages. Because of their high optical-to-THz radiation conversion efficiencies and reliability, the THz emitters made from moderately annealed LTG GaAs are a preferable choice for THz-TDS systems activated with femtosecond near-infrared lasers. On the other hand, the sensitivity of the pulsed THz detectors made from this material is by an order of magnitude worse than that for GaBiAs detectors – the best detecting devices for THz-TDS systems using lasers of the spectral range.

Acknowledgment This work was in part supported by the EU Marie Curie IRSES grant 230811, POLALAS. Dr. K. Bertulis is acknowledged for supplying the MBE grown layers for the experiments.

References

1. D. D. Nolte, J. Appl. Phys. Vol. 85, p. 6259–6289 (1999).
2. J. F. Whitaker, Mater. Sci. Eng., B 22, 1 p. 61–67 (1993).
3. A. Major, V. Barzda, P. A. E. Piunno, S. Musikhin and U.J. Krull, Opt. Express Vol. 14, 12 p. 5285–5294 (2006).
4. H. Liu, J. Nees and G. Mourou, Opt. Lett. Vol. 26, 21 p. 1723–1725 (2001).
5. S. Gupta, J. F. Whitaker and G. A. Mourou, IEEE J. Quantum Electron. Vol. 28, 10 p. 2464–2472 (1992).
6. K. Bertulis, A. Krotkus, G. Aleksejenko V. Pačebutas, R. Adomavičius, G. Molis, and S. Marcinkevičius, Appl. Phys. Lett. Vol. 88, 201112 (2006).
7. J. Sigmund, C. Sydlo, H. L. Hartnagel, N. Benker, H. Fuess, F. Rutz, T. Kleine-Ostmann, and M. Koch, Appl. Phys. Lett. Vol. 87, 252103 (2005).
8. F. Ospald, D. Maryenko, K. von Klitzing, D. C. Driscoll, M. P. Hanson, H. Lu, A. C. Gossard, and J. H. Smet, Appl. Phys. Lett. Vol 92, 131117 (2008).

9. D. C. Driscoll, M. Hanson, C. Kadow and A. C. Gossard, Appl. Phys. Lett. Vol 78, 12 p. 1703–1705 (2001).
10. A. Bičiūnas, A. Geižutis and A. Krotkus, Electron. Lett. Vol. 47, 2 p. 130–132 (2011).
11. SU Dankowski, D Streb, M Ruff, P Kiesel, M Kneissl, B Knüpfer, GH Döhler, UD Keil, CB Sørenson, AK Verma, Appl. Phys. Lett. Vol. 68, 1 p. 37–39 (1996).
12. JK Luo, H Thomas, DV Morgan, D Westwood, J. Appl. Phys. Vol. 79, 7 p. 3622–3629 (1996).
13. A. Krotkus, K. Bertulis, L. Dapkus, U. Olin, and S. Marcinkevičius, Appl. Phys. Lett. Vol. 75, 21 p. 3336–3338 (1999).
14. G. Molis, R. Adomavičius, A. Krotkus, K. Bertulis, L. Giniunas, J. Pocius and R. Danielius, Electron. Lett. Vol. 43, 3 p. 190–191 (2007).
15. M. C. Beard, G. M. Turner, and C. A. Schmuttenmaer, Phys. Rev. B Vol. 62, 15764 (2000).
16. G Vincent, D Bois, A Chantre, J. Appl. Phys. Vol. 53, 5 p. 3643–3649 (1982).
17. A Krotkus, K Bertulis, M Kaminska, K Korona, A Wolos, J Siegert, S Marcinkevicius, J-L Coutaz, IEE Proc. Optoelectron Vol. 149, 3 p. 111 – 115 (2002).
18. A. Urbanowicz, R. Adomavičius, A. Krotkus, V. L. Malevich, Semicond. Sci. Technol., Vol. 20, p. 1010 (2005).
19. R. Adomavičius, R. Šustavičiūtė and A. Krotkus, Springer proceedings in physics. ISSN 0930–8989. Vol. 119, p. 41–43. (2008).
20. TEM Staab, RM Nieminen, M Luysberg, J Gebauer, T Frauenheim, Physica B 340, p. 293–298 (2003).